Robust Hybrid Supervisory Control for Rendezvous and Docking of a Spacecraft

Bharani P. Malladi, Ricardo G. Sanfelice, Eric Butcher, and Jingwei Wang

Abstract—We consider the problem of rendezvous, proximity operations, and docking of an autonomous spacecraft. The problem can be conveniently divided into four phases: 1) rendezvous with angles-only measurements; 2) rendezvous with angle and range measurements; 3) docking phase; and 4) docked phase. Due to the different constraints, available measurements, and tasks to perform on each phase, we study this problem using a hybrid systems approach, in which the system has different modes of operation for which a suitable controller is to be designed. Following this approach, we characterize the family of individual controllers and the required properties they should induce to the closed-loop system to solve the problem within each phase of operation. Furthermore, we propose a supervisor that robustly coordinates the individual controllers so as to provide a solution to the problem. Due to the stringent mission requirements, the solution requires hybrid controllers that induce convergence, invariance, or asymptotic stability properties, which can be designed using recent techniques in the literature of hybrid systems. In addition, we outline specific controller designs that appropriately solve the control problems for individual phases and validate them numerically.

I. Introduction

There is a pressing need to better understand and control the dynamics of relative satellite motion (i.e., the motion of one satellite with respect to one or more other satellites) for close-proximity missions. These missions include both formation flying missions and rendezvous. The relative motion between two or more satellites in close proximity are often modeled assuming a circular chief orbit and a deputy orbit linearized about the chief's motion. This results in the wellknown Clohessy-Wiltshire-Hill (CWH) equations [1], [2], which is a linear time-invariant model. Guidance, closed-loop control, and navigation algorithms for relative satellite trajectories must be designed taking into account both mission requirements/constraints and the natural orbital dynamics of the system. In addition, control of the satellites must often be accomplished in an optimal fashion, where trajectory time and/or fuel expenditure are of concern. Feedback control solutions may involve LQR control [3], time-varying gain control [4], output tracking schemes that successfully reject disturbances [5], and model predictive control strategies [6], [7], [8].

In this paper, we apply the divide-and-conquer approach enabled by hybrid feedback control to the problem of

- B. P. Malladi, E. Butcher, and J. Wang are with the Department of Department of Aerospace and Mechanical Engineering, University of Arizona, 1130 N Mountain Ave, Tucson, AZ, 85721. email: malladi@email.arizona.edu, email: ebutcher@email.arizona.edu, email: iwwang@email.arizona.edu
- R. G. Sanfelice is with the Department of Computer Engineering, University of California at Santa Cruz, 1156 High Street MS:SOE3, Santa Cruz, CA 95064. email: ricardo@ucsc.edu

Research by R. G. Sanfelice partially supported by NSF Grants no. ECS-1150306 and CNS-1544396, and by AFOSR Grant no. FA9550-16-1-0015.

¹This submission is part of an invited session proposal focusing on this problem and featuring papers proposing solutions using different tools.

rendezvous, proximity operations, and docking of an autonomous spacecraft modeled using the CWH equations, which are widely used in the literature of spacecraft control. As a difference to switching systems approaches, hybrid control allows for the implementation of hysteresis in the control strategy. As formulated in [9], this problem consists of the following four main phases: 1) rendezvous with angles-only measurements; 2) rendezvous with range and angle measurements; 3) docking phase; and 4) docked phase. The state constraints, available measurements, as well as the tasks to perform are different for each of the phases. This change in the specifications and in the function defining the measurements (namely, the output function) lead to a nonsmooth dynamical system. Due to the interest in a feedback controller that does not exhibit chattering, can be systematically designed in a modular fashion, and guarantees robust stability properties, we propose a hybrid systems approach. In this method, the system has different modes of operation, hence, the design of both individual controllers for each mode, as well as, the algorithm that supervises them is outlined below. More precisely, we contribute to the problem of rendezvous, proximity operations, and docking of an autonomous spacecraft by

- Characterizing the family of individual controllers and the required properties they should induce to the closedloop system to solve the problem within each phase of operation.
- Designing a supervisor that robustly coordinates the individual controllers so as to provide a solution to the problem.
- Providing specific controller designs that appropriately solve the control problems for individual phases and validate them numerically.

The remainder of the paper is organized as follows. In Section II, the notation used throughout the paper is defined and needed background material on hybrid controllers is provided. The problem of interest is formalized in Section III. A general hybrid feedback control solution is presented in Section IV, where a family of individual controllers is characterized and a supervisor is designed. Specific design and numerical simulations are given in Section V. Due to space limitations, additional details and the proof of the main result will be published elsewhere.

II. PRELIMINARIES

A. Notation

The following notation and definitions are used throughout the paper. \mathbb{R}^n denotes n-dimensional Euclidean space. \mathbb{R} denotes the real numbers. \mathbb{Z} denotes the integers. $\mathbb{R}_{\geq 0}$ denotes the nonnegative real numbers, i.e., $\mathbb{R}_{\geq 0} = [0, \infty)$. \mathbb{N} denotes the natural numbers including 0, i.e., $\mathbb{N} = \{0, 1, \ldots\}$. \mathbb{R} denotes the open unit ball in a Euclidean space. Given a set

 S, \overline{S} denotes its closure. Given a vector $x \in \mathbb{R}^n$, |x| denotes the Euclidean vector norm. Given a closed set $S \subset \mathbb{R}^n$ and a point $x \in \mathbb{R}^n$, $|x|_S := \inf_{y \in S} |x - y|$. Given sets S_1, S_2 subsets of \mathbb{R}^n , $S_1+S_2:=\{x_1+x_2:x_1\in S_1,x_2\in S_2\}$. The equivalent notation $[x^\top\ y^\top]^\top$, and (x,y) is used for vectors. $S_{(+)}$ denotes the set of positive definitive matrices.

B. Hybrid controllers

In this paper, we consider stabilization problems for nonlinear control systems of the form

$$\mathcal{P}: \quad \dot{\eta} = f_P(\eta, u), \quad y = h_P(\eta) \quad (\eta, u) \in C_P \times \mathcal{U}_P \quad (1)$$

where $\mathcal{U}_P \subset \mathbb{R}^{m_P}$ is a set defining the available input values, $C_P \subset \mathbb{R}^{n_P}$ is a set where the plant state $\eta \in \mathbb{R}^{n_P}$ is allowed to evolve, $f_P:C_P\times\mathcal{U}_P\to \mathbb{R}^{n_P}$ is a function defining the continuous dynamics, and $h_P:C_P o\mathbb{R}^{n_P}$ is the output function. A hybrid controller $\mathcal{H}_c = (C_c, f_c, D_c, G_c, h_c)$ takes the form (see [10], [11])

$$\mathcal{H}_{c}: \begin{cases} y_{c} = h_{c}(u_{c}, x_{c}) \\ \dot{x}_{c} = f_{c}(u_{c}, x_{c}) & (u_{c}, x_{c}) \in C_{c} \\ x_{c}^{+} \in G_{c}(u_{c}, x_{c}) & (u_{c}, x_{c}) \in D_{c} \end{cases}$$
 (2)

 $\mathcal{Y}_c \subset \mathbb{R}^{r_c}$ denotes the controller output, $x_c \in \mathbb{R}^{n_c}$ is the controller state, the sets C_c and D_c define regions where the controller state can flow and jump, respectively, $h_c: C_c \rightarrow$ \mathcal{Y}_c defines the output of the controller and $f_c: C_c \to \mathbb{R}^{n_c}$ the flows, while $G_c:D_c\rightrightarrows\mathbb{R}^{n_c}$ is a map that defines how the controller state x_c is updated at jumps. When $\mathcal{Y}_c = \mathcal{U}_P$ and system (1) is controlled by \mathcal{H}_c via the interconnection conditions $u_c = y$, and $u = y_c$, the resulting hybrid closedloop system \mathcal{H}_{cl} is given by

$$\mathcal{H}: \left\{ \begin{array}{rcl} \dot{\eta} & = & f_P(\eta, h_c(h_P(\eta), x_c)) \\ \dot{x}_c & = & f_c(h_P(\eta), x_c) \end{array} \right\} =: F(x) \\ \eta^+ & = & \eta \\ x_c^+ & \in & G_c(h_P(\eta), x_c) \end{array} \right\} =: G(x) \\ (\eta, x_c) \in D$$

where, $C := \{(\eta, x_c) : (\eta, h_c(h_P(\eta), x_c)) \in C_P \times \mathcal{U}_P, (h_P(\eta), x_c) \in C_c\}, D := \{(\eta, x_c) : (h_P(\eta), x_c) \in D_c\}.$ If \mathcal{H}_c is such that C_c and D_c are closed, f_c and h_c are continuous, G_c is outer semicontinuous and locally bounded, and $G_c(x_c, u_c)$ is a nonempty subset of $\mathbb{R}^{n_c} \times \mathbb{R}^{m_c}$ for all $(x_c, u_c) \in D_c$, then \mathcal{H}_c is said to be well-posed. Note that this interconnection is well-posed when its data satisfies the hybrid basic conditions. For more details on the definitions of hybrid time domain, hybrid arc, hybrid basic conditions, asymptotic stability and well-posedness of hybrid system see [11].

III. PROBLEM DESCRIPTION

We consider a model of the chaser spacecraft given by the so-called Clohessy-Wiltshire equations, namely,

$$\ddot{x} - 2n\dot{y} - 3n^2x = \frac{F_x}{m_c}$$

$$\ddot{y} + 2n\dot{x} = \frac{F_y}{m_c}$$

$$(4)$$

where (x, y) and (\dot{x}, \dot{y}) are the planar position and velocity, respectively, F_x and F_y are the control forces in the x and y directions, respectively, m_c the mass of the chaser, and $n := \sqrt{\frac{\mu}{r_0^3}}$ where μ is the gravitational parameter of the Earth and r_o is the orbit radius of the target spacecraft. The target spacecraft is located at (x, y) = (0, 0) and has mass m_t . The state space representation of (4) is given by

$$\dot{\eta} = A\eta + Bu \tag{5}$$

where $\eta:=\begin{bmatrix}x&y&\dot{x}&\dot{y}\end{bmatrix}^{\top}\in\mathbb{R}^4$ is the state vector, $u:=\begin{bmatrix}F_x&F_y\end{bmatrix}^{\top}\in\mathbb{R}^2$ is the input vector, and

$$A := \begin{bmatrix} 0 & 0 & 1 & 0 \\ 0 & 0 & 0 & 1 \\ 3n^2 & 0 & 0 & 2n \\ 0 & 0 & -2n & 0 \end{bmatrix}, \qquad B := \begin{bmatrix} 0 & 0 \\ 0 & 0 \\ \frac{1}{m_c} & 0 \\ 0 & \frac{1}{m_c} \end{bmatrix}$$

are the state and input matrices, respectively. The relative position between the chaser and the target is represented by $\rho(x,y) := \sqrt{x^2 + y^2}$. Let $\mathcal{N}^n(0,\sigma^2)$ be the set of measurable functions in an n-dimensional Euclidean space with Gaussian distribution having zero mean and variance σ^2 . We are ready to state the problem to solve.

Problem 1: Given positive constants m_c , m_t , μ , r_o , u_{max} , $ho_{\max} >
ho_r >
ho_d$, \overline{V}, V_{\max} , σ_1 , σ_2 , σ_3 , σ_4 , $t_f > t_e$, $\theta \in [0, \frac{\pi}{2})$, and $(x_p, y_p) \in \mathbb{R}^2$, design a feedback controller that measures $y = h(\eta) + v$

and assigns u such that for every initial condition

$$\eta_0 \in \mathcal{M}_0 := \left\{ \eta \in \mathbb{R}^4 : \rho(x, y) \in [0, \rho_{\max}], \rho(\dot{x}, \dot{y}) \in [0, \overline{V}] \right\}$$

of the chaser with dynamics as in (5) under the constraints

• The control signal $t \mapsto u(t)$ satisfies the "maximum thrust" constraint

$$\sup_{t\geq 0} \max\{|F_x(t)|,|F_y(t)|\} \leq u_{\max}$$
 namely, for each $t\geq 0,$

$$u(t) \in \mathcal{U}_P := \{ u \in \mathbb{R}^2 : \max\{|F_x|, |F_y|\} \le u_{\max} \}$$
 (6)

• For each $\eta \in \mathcal{M}_1 := \left\{ \eta \in \mathbb{R}^4 : \rho(x,y) \in [\rho_r,\infty) \right\}$, only angle measurements² are available, namely,

$$h(\eta) = \arctan\left(\frac{y}{x}\right)$$

 $h(\eta) = \arctan\left(\frac{y}{x}\right)$ where $\arctan: \mathbb{R} \to [-\pi,\pi]$ is the four-quadrant inverse tangent, and $v \in \mathcal{N}(0,\sigma_1^2)$;

• For each $\eta \in \mathcal{M}_2 := \{ \eta \in \mathbb{R}^4 : \rho(x,y) \in [\rho_d, \rho_r) \},$ angle and range measurements are available, namely,

$$h(\eta) = \begin{bmatrix} \arctan\left(\frac{y}{x}\right) \\ \sqrt{x^2 + y^2} \end{bmatrix} \tag{7}$$

and $v \in \mathcal{N}^2(0, \sigma_2^2)$;

• For each $\eta \in \overline{\mathcal{M}}_3^a := \{ \eta \in \mathbb{R}^4 : \rho(x,y) \in [0,\rho_d) \},$ angle and range measurements are available, that is, we have h as in (7) and $v \in \mathcal{N}^2(0, \sigma_3^2)$ while, in addition, if $\eta \in \mathcal{M}_3^a \cap \mathcal{M}_3^b$, where

$$\mathcal{M}_{3}^{b}(\theta) \coloneqq \left\{ \eta \in \mathbb{R}^{4} : \begin{bmatrix} \sin(\theta/2) & \cos(\theta/2) \\ \sin(\theta/2) & -\cos(\theta/2) \end{bmatrix} \begin{bmatrix} x \\ y \end{bmatrix} \leq \begin{bmatrix} 0 \\ 0 \end{bmatrix} \right\}$$

namely, the position state is in a cone with aperture θ

²To overcome the discontinuities associated with angle calculations, we embed the angle on a unit circle, in other words we consider line of sight (LOS) measurements given by, $h(\eta) := \begin{vmatrix} \frac{x}{\rho(x,y)} & \frac{y}{\rho(x,y)} \end{vmatrix}^{\top}$.

centered about the x axis, then the following constraint on closing/approaching velocity is satisfied:

$$\eta \in \mathcal{M}_3^c := \left\{ \eta \in \mathbb{R}^4 : \rho(\dot{x}, \dot{y}) \le V_{\text{max}} \right\}.$$

where,
$$\rho(\dot{x}, \dot{y}) := \sqrt{\dot{x}^2 + \dot{y}^2}$$
.

When the chaser docks to the target (docked-phase), the chaser-target dynamics are given as in (5) with m_c+m_t in place of m_c under the constraint (6) and with position measurements relative to a partner at location (x_p,y_p) are available, namely,

$$h(\eta) \hspace{-0.1cm} = \hspace{-0.1cm} \begin{bmatrix} \arctan\left(\frac{r_x(x)}{r_y(y)}\right) \\ \sqrt{r_x(x)^2 + r_y(y)^2} \end{bmatrix}, \; r_x(x) = x - x_p, \; r_y(y) = y - y_p$$

and $v \in \mathcal{N}^2(0, \sigma_4^2)$.

The following holds for the η -component $t\mapsto \eta(t)$ of each solution to the closed-loop system: for some $t_{2f}< t_{3f}< t_{4f}$ such that $t_{3f}\leq t_e,\ t_{4f}\leq t_f$, we have

- 1) $\eta(t_{2f}) \in \mathcal{M}_3^a \cap \mathcal{M}_3^b$ and $\rho(x(t_{2f}), y(t_{2f})) = \rho_d$; namely, the chaser reaches the cone first;
- 2) $\eta(t_{3f}) \in \mathcal{M}_3^c = \{ \eta \in \mathbb{R}^4 : \eta = 0 \}$; namely, the chaser docks on the target next, no later than t_{3f} time units;
- 3) $\eta(t_{4f}) \in \mathcal{M}_4$, where $\mathcal{M}_4 := \{ \eta \in \mathbb{R}^4 : x = x_p, y = y_p, \dot{x} = \dot{y} = 0 \}$; namely, the docked chaser (or chaser-target) reach the partner location no later than t_{4f} time units. \triangle

Remark 3.1: The values of the constants m_c , m_t , μ , r_o , $u_{\rm max}$, and (x_p,y_p) are imposed by the vehicles and their environment. The constants $\rho_{\rm max}$, ρ_r , ρ_d , \overline{V} , $V_{\rm max}$, θ , t_f , and t_e are imposed by the mission and the desired performance. The values used for the simulations in Section V were provided by the organizers of the invited session proposal that this paper is part of.

To define the dynamics of the systems to control under the above constraints, we define the following functions and sets: with $\varepsilon \in (0,\theta), \, \delta_{2b}^* > 0$,

$$\mathcal{M} := \mathcal{M}_2 \cup \mathcal{M}_3^a = \left\{ \eta \in \mathbb{R}^4 : \rho(x, y) \in [0, \rho_r) \right\}$$

$$\mathcal{X}_{los} := \mathcal{M}_3^a \cap \mathcal{M}_3^b(\theta), \qquad \mathcal{X}_{los}^{\varepsilon} := \mathcal{M}_3^a \cap \mathcal{M}_3^b(\theta - \varepsilon)$$

$$\mathcal{X}_{los}^{\varepsilon \delta} := \left((\mathcal{X}_{los}^{\varepsilon} + \delta_{2b}^* \mathbb{B}) \cap \mathcal{M}_3^b(\theta - \varepsilon) \right) \setminus \mathcal{X}_{los}^{\varepsilon},$$

$$h_1(\eta) := \arctan\left(\frac{y}{x}\right) \qquad \forall \eta \in \mathcal{M} \cup \mathcal{M}_1$$

$$h_2(\eta) := \begin{bmatrix} h_1(\eta) \\ \sqrt{x^2 + y^2} \end{bmatrix} \qquad \forall \eta \in \mathcal{M}$$

$$h_3(\eta) := h_2(\eta) \qquad \forall \eta \in \mathcal{M}$$

$$h_4(\eta) := \begin{bmatrix} \arctan\left(\frac{r_x(x)}{r_y(y)}\right) \\ \sqrt{r_x(x)^2 + r_y(y)^2} \end{bmatrix} \qquad \forall \eta \in \mathcal{M}$$

Then, the dynamics of the chaser are given by the plant

$$\dot{\eta} = A\eta + Bu
y_a = h_P(\eta) := \begin{cases} \begin{bmatrix} h_1(\eta) \\ h_0(\eta) \end{bmatrix} & \text{if } \eta \in \mathcal{M}_1 \\ h_2(\eta) & \text{if } \eta \in \mathcal{M} \end{cases}$$

$$(\eta, u) \in C_P \times \mathcal{U}_P$$

where $C_P := (((\mathcal{M} \cup \mathcal{M}_1) \setminus \mathcal{X}_{los}) \cup (\mathcal{X}_{los} \cap \mathcal{M}_3^c))$. The virtual output function h_0 is defined to capture the lack of range measurements when in \mathcal{M}_1 : for some small $\gamma > 0$,

 $h_0(\eta)$ is zero for each $\eta \in \mathcal{M}_1 \setminus (\mathcal{M} + \gamma \mathbb{B})$, and equal to $\sqrt{x^2 + y^2}$ for each $\eta \in \mathcal{M}$. Similarly, the constrained dynamics of the chaser-target are

$$\begin{array}{rcl}
\dot{\eta} & = & A\eta + B_R u \\
y_b & = & h_R(\eta) := h_3(\eta)
\end{array} \right\} \qquad (\eta, u) \in C_R \times \mathcal{U}_P \quad (9)$$

where

$$B_R := egin{bmatrix} 0 & 0 & 0 \ 0 & 0 \ rac{1}{m_c + m_t} & 0 \ 0 & rac{1}{m_c + m_t} \end{bmatrix}, \quad C_R := \mathcal{M}.$$

IV. GENERAL HYBRID FEEDBACK CONTROL STRATEGY

We propose an algorithm that supervises multiple hybrid controllers that are designed to cope with the individual constraints and to satisfy the desired temporal properties. The supervising algorithm is modeled as a hybrid system, which we denote \mathcal{H}_s , and is in charge of supervising the following individual hybrid controllers:

- Hybrid controller for rendezvous from distances far from target (Phase I): this controller is denoted $\mathcal{H}_{c,1}$ and its goal is to steer the chaser to a point in the interior of \mathcal{M} , in particular, from points in the compact set $\mathcal{M}_1 \cap \mathcal{M}_0$.
- Hybrid controller for rendezvous in close-proximity to target (Phase II): this controller is denoted $\mathcal{H}_{c,2}$ and its goal is to steer the chaser to a point in the interior of \mathcal{X}_{los} , in particular, from points in \mathcal{M}_2 .
- Hybrid controller for docking to target (Phase III): this controller is denoted $\mathcal{H}_{c,3}$ and its goal is to steer the chaser to nearby $\eta = 0$ from points in $\mathcal{M}_2 \cup \mathcal{M}_3^a$.
- Hybrid controller for relocation of target (Phase IV): this controller is denoted $\mathcal{H}_{c,4}$ and its goal is to steer the chaser-target from nearby \mathcal{M}_3^c to a neighborhood of the partner position (x_p, y_p) .

The operations described above are subject to the constraints stated in Problem 1. Each of the hybrid controllers operates in specific regions of the state space. These regions along with the goals of the individual hybrid controllers are formalized next. Note that the tasks performed by the controllers $\mathcal{H}_{c,3}$ and $\mathcal{H}_{c,4}$ are practical, in the sense that the trajectories η are steered from and to neighborhoods of the desired sets respectively.

We have the following result.

Theorem 4.1: Given the parameters listed in **Problem 1** and subject to the constraints therein, suppose there exist positive constants δ_1 , δ_1^* , δ_2 , δ_{2a}^* , δ_{2b}^* , δ_3 , δ_3^* , δ_4 , δ_4^* , and ε , such that $\delta_1 \in (0, \min\{\delta_1^*, \rho_r - \rho_d\})$, $\delta_2 \in (0, \delta_{2a}^*)$, $\delta_3^* \in (0, \rho_d)$, $\delta_3 \in (0, \delta_3^*)$, closed sets \mathcal{A}_1 , \mathcal{A}_2 , and \mathcal{A}_4 satisfying

$$\begin{array}{lll}
\mathcal{A}_{1} + \delta_{1}^{*}\mathbb{B} & \subset & \mathcal{M}, \\
\mathcal{A}_{2} + \delta_{2a}^{*}\mathbb{B} & \subset & \mathcal{X}_{los}^{\varepsilon\delta}, \\
\mathcal{A}_{4} + \delta_{4}\mathbb{B} & \subset & (x_{p}, y_{p}, 0, 0) + \delta_{4}^{*}\mathbb{B} \\
(x_{p}, y_{p}, 0, 0) & \in & \mathcal{A}_{4}
\end{array} (10)$$

and

- 1) A well-posed hybrid controller $\mathcal{H}_{c,1}$ rendering $\mathcal{A}_1 + \delta_1 \mathbb{B}$ finite-time attractive from $\mathcal{M}_1 \cap \mathcal{M}_0$ within T_1 seconds;
- 2) A well-posed hybrid controller $\mathcal{H}_{c,2}$ rendering $\mathcal{A}_2 + \delta_2 \mathbb{B}$ finite-time attractive from

$$\left\{ \eta \in \mathbb{R}^4 : \rho(x,y) \in [0, \rho_r - \delta_1] \right\}$$

within T_2 seconds;

- 3) A well-posed hybrid controller $\mathcal{H}_{c,3}$ capable of
 - a) steering η from $A_2 + \delta_2 \mathbb{B}$ to $\mathcal{X}_{los}^{\varepsilon}$ within T_{3a} seconds:
 - b) rendering $\mathcal{X}_{los}^{\varepsilon} \cup \mathcal{X}_{los}^{\varepsilon\delta}$ forward invariant;
 - c) steering η from $\mathcal{X}_{los}^{\varepsilon}$ to $\mathcal{A}_3 + \delta_3 \mathbb{B}$ within T_{3b} seconds, where, $\mathcal{A}_3 := \{(0,0,0,0)\}.$
- 4) A well-posed hybrid controller $\mathcal{H}_{c,4}$ rendering $\mathcal{A}_4 + \delta_4 \mathbb{B}$ finite-time attractive from $\mathcal{A}_3 + \delta_3 \mathbb{B}$ within T_4 seconds and \mathcal{A}_4 asymptotically stable, with the basin of attraction containing $\mathcal{A}_4 + \delta_4 \mathbb{B}$.
- 5) $T_1 + T_2 + T_3 \le t_e$ and $T_4 \le t_f t_e$.

Then, there exists a supervisor \mathcal{H}_s that solves³ **Problem 1** and renders the set \mathcal{A}_4 asymptotically stable with basin of attraction containing \mathcal{M}_0 when projected to the η component of the state space. Furthermore, the set \mathcal{A}_4 is semiglobally practically robustly asymptotically stable for the closed-loop system with quantifiable margin of robustness.

To establish the properties in Theorem 4.1, we explicitly construct a supervisor \mathcal{H}_s guaranteeing the stated properties. We start by characterizing the properties of the individual hybrid controllers.

A. Hybrid Controller for Phase I

The hybrid controller $\mathcal{H}_{c,1}$ renders an inflation of the closed set \mathcal{A}_1 finite-time attractive for the solution components η starting from $\mathcal{M}_1 \cap \mathcal{M}_0$. The inflation is given by the set $\mathcal{A}_1 + \delta_1 \mathbb{B}$ with $\delta_1 \in (0, \delta_1^*)$, where $\delta_1^* > 0$ satisfies (10). Namely, the basin of attraction induced by $\mathcal{H}_{c,1}$ in η space is \mathcal{B}_1^{η} and contains $\mathcal{M}_1 \cap \mathcal{M}_0$. When this property holds, the components η of solutions with $\mathcal{H}_{c,1}$ will reach \mathcal{M} in finite time due to \mathcal{A}_1 being in the interior of \mathcal{M} . The neighborhood of size δ_1^* in (10) enables the supervisor to use measurements given by h_2 to detect when η is inside \mathcal{M} . For this purpose, we define the set of η points that trigger switches in the supervisor from using $\mathcal{H}_{c,1}$ to using $\mathcal{H}_{c,2}$ as

$$\begin{split} D_{12} &:= \left\{ \eta \in \mathbb{R}^4 \ : \ \rho(x,y) \in [0,\rho_r - \overline{\delta}_1 \ \right\}] \\ \text{where, } \overline{\delta}_1 &\in (0, \min\{\delta_1^*, \rho_r - \rho_d\}) \text{ is such that} \\ \mathcal{A}_1 &+ \delta_1 \mathbb{B} \subset D_{12} \text{ and } \mathcal{M} \setminus D_{12} \subset \mathcal{M}_2. \end{split}$$

The latter condition guarantees that switches from using $\mathcal{H}_{c,1}$ to using $\mathcal{H}_{c,2}$ occur inside \mathcal{M}_2 .

Due to the presence of noise or wrong initializations, switches back to $\mathcal{H}_{c,1}$ may need to be triggered. Using measurements given by h_2 , such switches will occur nearby the boundary of \mathcal{M} and away from D_{12} . We refer to this set as the recovery set of the supervisor and define it as

$$D_{r1} := \left\{ \eta \in \mathbb{R}^4 : \rho(x,y) \in [\rho_r - \delta_{r1}, \rho_r] \right\}$$
 where, $\delta_{r1} \in (0, \overline{\delta}_1)$. Figure 1 sketches these constructions.

B. Hybrid Controller for Phase II

The hybrid controller $\mathcal{H}_{c,2}$ renders an inflation of the closed set \mathcal{A}_2 finite-time attractive for the solution components η starting from D_{12} . The inflation is given by the set $\mathcal{A}_2 + \delta_2 \mathbb{B}$ with $\delta_2 \in (0, \delta_{2a}^*)$, where $\delta_{2a}^* > 0$ satisfies

$$\mathcal{A}_2 + \delta_{2a}^* \mathbb{B} \subset \mathcal{X}_{los}^{\varepsilon \delta} \tag{11}$$

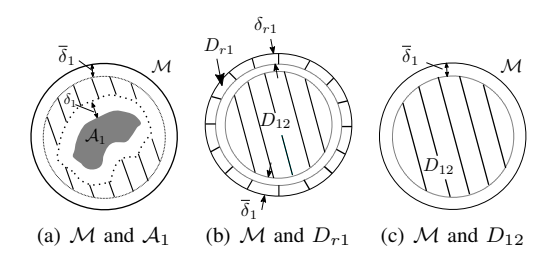


Fig. 1. Set constructions for $\mathcal{H}_{c,1}$.

for some $\delta_{b2}^*>0$. Namely, the basin of attraction induced by $\mathcal{H}_{c,2}$ in η space is \mathcal{B}_2^{η} and contains D_{12} . When this property holds, the components η of such solutions will reach in finite time a nearby point outside \mathcal{X}_{los} that is within the cone, namely, a point in $\mathcal{X}_{los}^{\varepsilon\delta}$. By steering η to a point outside of \mathcal{X}_{los} , the hybrid controller $\mathcal{H}_{c,2}$ does not need to satisfy the maximum closing velocity constraint imposed within \mathcal{X}_{los} (this task is relayed to $\mathcal{H}_{c,3}$). Unlike the construction of $\mathcal{H}_{c,1}$, the supervisor will trigger switches that stop using $\mathcal{H}_{c,2}$ and start using $\mathcal{H}_{c,3}$ when η in $\mathcal{A}_2 + \delta_2\mathbb{B}$. Then, we define

$$D_{23} := \overline{\mathcal{A}_2 + \delta_2 \mathbb{B}}.$$

Switches back to $\mathcal{H}_{c,2}$ may need to be triggered due to the presence of perturbations or wrong initializations. Let

$$\mathcal{X}_{los}^{\delta} := \left(\left(\mathcal{X}_{los} + \delta_{2b}^* \mathbb{B} \right) \cap \mathcal{M}_3^b(\theta) \right) \setminus \mathcal{X}_{los}.$$

Using measurements given by h_3 , such switches will occur right outside of $\mathcal{X}_{los} \cup \mathcal{X}_{los}^{\delta}$. Then, the recovery set of the supervisor for this controller is given by

$$D_{r2} := \overline{\mathcal{M} \setminus (\mathcal{X}_{los} \cup \mathcal{X}_{los}^{\delta})}.$$

Figure 2 sketches these constructions.

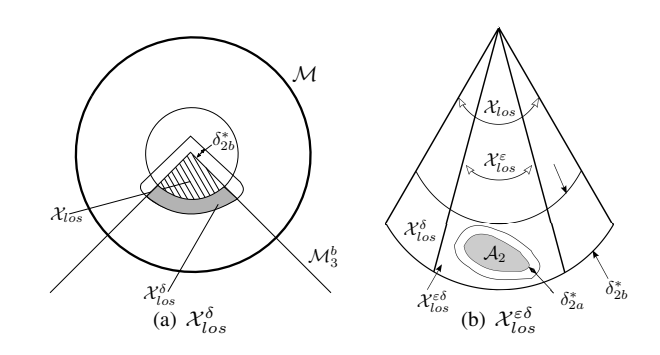


Fig. 2. Set constructions for $\mathcal{H}_{c,2}$ and $\mathcal{H}_{c,3}$.

C. Hybrid Controller for Phase III

The hybrid controller $\mathcal{H}_{c,3}$ steers η components of the solutions from $\mathcal{A}_2 + \delta_2 \mathbb{B}$ to $\mathcal{X}^{\varepsilon}_{los}$ in finite time, render $\mathcal{X}^{\varepsilon}_{los} \cup \mathcal{X}^{\varepsilon\delta}_{los}$ forward invariant, and an inflation of the set \mathcal{A}_3 finite-time attractive. The inflation is given by the set $\mathcal{A}_3 + \delta_3 \mathbb{B}$. This controller enforces the maximum closing velocity constraint within \mathcal{X}_{los} as well. The finite separation between $\mathcal{A}_2 + \delta_2 \mathbb{B}$ and \mathcal{X}_{los} makes this task feasible as this controller will have time to slow down the chaser before reaching $\mathcal{X}^{\varepsilon}_{los}$ if needed. Then, switches of the supervisor to $\mathcal{H}_{c,4}$ are triggered when η is in

$$D_{34} := (\mathcal{A}_3 + \delta_3 \mathbb{B}) \cap \mathcal{X}_{los}^{\varepsilon}$$

which collects points that are δ_3 -close to \mathcal{A}_3 with $\delta_3 \in (0, \delta_3^*)$, where δ_3^* is such that

$$(\mathcal{A}_3 + \delta_3^* \mathbb{B}) \cap \mathcal{X}_{los} \cap \mathcal{X}_{los}^{\delta} = \emptyset$$

 $^{^3}$ Modulo the fact that the η converges to a δ_4^* neighborhood of the partner position.

which is guaranteed by picking δ_3^* small enough. Figure 2 and Figure 3 sketch these constructions.

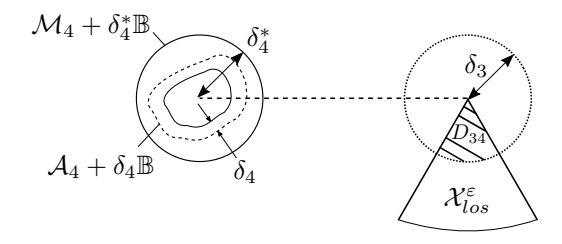


Fig. 3. Set constructions for $\mathcal{H}_{c,3}$ and $\mathcal{H}_{c,4}$.

D. Hybrid Controller for Phase IV

The hybrid controller $\mathcal{H}_{c,4}$ performs a maneuver in finite time from points in D_{34} to nearby \mathcal{M}_4 which is an isolated point. Due to the presence of noise, steering the state to an isolated point is not practical, and hence we design $\mathcal{H}_{c,4}$ to steer η in finite time to a point in $\mathcal{M}_4 + \delta_4^* \mathbb{B}$, where $\delta_4^* > 0$.

For this purpose, we propose a controller that renders the set A_4 asymptotically stable and the set $A + \delta_4 \mathbb{B}$ finite-time stable, where $\delta_4 > 0$ is such that

$$\mathcal{A}_4 + \delta_4 \mathbb{B} \subset \mathcal{M}_4 + \delta_4^* \mathbb{B}, \qquad \mathcal{M}_4 \subset \mathcal{A}_4$$

In particular, this construction assures some robustness to small perturbations. Figure 3 sketches these constructions.

E. Supervisor

The supervisor employs the constructions Sections IV-A-IV-D to implement the following logic:

- Apply $\mathcal{H}_{c,1}$ when η is in $(\mathcal{M}_1 \cup \mathcal{M}) \setminus D_{12}$;
- While applying $\mathcal{H}_{c,1}$, switch to applying $\mathcal{H}_{c,2}$ if η is in
- Apply $\mathcal{H}_{c,2}$ in $\overline{\mathcal{M} \setminus D_{r1}}$; While applying $\mathcal{H}_{c,2}$, switch to applying $\mathcal{H}_{c,1}$ if η is in
- While applying $\mathcal{H}_{c,2}$, switch to applying $\mathcal{H}_{c,3}$ if η is in
- Apply $\mathcal{H}_{c,3}$ if η is in $\mathcal{X}_{los}^{\varepsilon} \cup \mathcal{X}_{los}^{\varepsilon\delta}$; While applying $\mathcal{H}_{c,3}$, switch to applying $\mathcal{H}_{c,2}$ if η is in
- While applying $\mathcal{H}_{c,3}$, switch to applying $\mathcal{H}_{c,4}$ if η is in
- Apply $\mathcal{H}_{c,4}$ and let η converge to $\mathcal{A}_4 + \delta_4 \mathbb{B}$.

A hybrid system implementing this logic is defined next. Let $q \in Q := \{1, 2, 3, 4\}$ be a logic state denoting the controller currently being applied. Then, for the nominal case, the hybrid supervisor has the following dynamics:

$$\dot{q} = 0 \qquad (q, u_s) \in C_s$$

$$q^+ = G_s(q, u_s) \qquad (q, u_s) \in D_s$$

with output $y_s = \kappa_c(q, u_s)$, where

- $\kappa_c(q,\cdot)$ is the output of $\mathcal{H}_{c,q}$;
- $u_s = y_a$ when $q \neq 4$, and $u_s = y_b$ when q = 4 note that when $\eta \in \mathcal{M}$ and $q \neq 4$, $u_s = \eta$ in the nominal

•
$$C_s := \bigcup_{q \in Q} (\{q\} \times C_q)$$
 and $D_s = \bigcup_{q \in Q} (\{q\} \times D_q)$

where

$$C_{1} := \overline{(\mathcal{M}_{1} \cup \mathcal{M}) \setminus D_{12}}, \quad C_{2} := \overline{\mathcal{M} \setminus D_{r1}}$$

$$C_{3} := \mathcal{X}_{los}^{\varepsilon} \cup \mathcal{X}_{los}^{\varepsilon\delta}, \quad C_{4} := \mathcal{M} \cup \mathcal{M}_{1}$$

$$D_{1} := D_{12}, \quad D_{2} := D_{r1} \cup D_{23}$$

$$D_{3} := D_{r2} \cup D_{34}, \quad D_{4} := \emptyset$$

• the jump map G_s is defined as

$$G_s(q,u_s)\!=\!\left\{\begin{array}{ll} 2 & \text{if } q=1, \eta \in D_{12}, \text{or } q=3, \! \eta \in D_{r2} \\ 1 & \text{if } q=2, \eta \in D_{r1} \\ 3 & \text{if } q=2, \eta \in D_{23} \\ 4 & \text{if } q=3, \eta \in D_{34} \end{array}\right.$$

Due to space limitations, proof of Theorem 4.1 will be published elsewhere.

V. SPECIFIC DESIGNS AND SIMULATIONS

In Phase-I, since the chaser is relatively far away from the target, with angle only measurement, the system in (8) is unobservable [12]. Following the results in [13], we add high-order nonlinear terms to (8) to attain observability (output feedback could be an alternate approach). Therefore in Phase I, to estimate the state η from angle (α) measurement only, a sequential Kalman filter on the resulting plant with the feedforward term (following [14]) $\Gamma(\eta) :=$ $\frac{\mu}{r_o^4} \begin{bmatrix} 0 & 0 & -3x^2 + \frac{3}{2}y^2 & 3xy \end{bmatrix}^{\top}$ is implemented. An LQR feedback controller that compensates for the higher-order nonlinear terms is designed, to which state estimates are fed. In Phase-II, we exploit the ideas in [3] (in particular, the change of coordinates), where a proportional-derivative control law that guides the chaser to dock with the target at a desired docking direction ($\alpha = \alpha^*$) and position ($\rho = \rho^*$) is proposed. A logic variable h is introduced to handle the topological obstruction of stabilizing a set on a manifold and designed a logic-based hybrid controller that robustly steers the chaser (either clockwise or counter-clockwise) to reach a point in $\mathcal{X}_{los}^{\varepsilon\delta}$. In Phase-III, a hybrid controller that unites local and "global" controllers is implemented. This controller is designed to induce forward invariance and to satisfy the closing speed constraints for the chaser. In Phase-IV, a simple LQR controller is designed. Due to space limitations, additional details for each of the individual controllers will be published elsewhere.

A. Simulation results

We use $n=\sqrt{\frac{\mu}{r_o{}^3}}, \mu=3.986\times 10^{14}\frac{m^3}{s^2}, r_o=7100000m,$ $m_c=500Kg$ and $m_t=2000Kg$ in the simulations. In the problem definition provided to us for this invited session, the chaser starts at a distance of no more than $\rho_{\rm max} = 10 Km$ away from the target and has to reach it in worst-case time of $t_e = 4hr$. Once docked the chaser-target has to reach a relocation position with range $\rho(x,y) = 20Km$, which is 10Km away from the partner spacecraft in worst-case time of $t_f = 12hr$.

With these mission parameters, simulations for the entire closed-loop system are performed for the chaser starting from $\eta \in \mathcal{M}_0 \cap \mathcal{M}_1$, which corresponds to various initial conditions in the 10Km radius with a initial velocity $\rho(\dot{x}(0,0),\dot{y}(0,0)) \in [0,0.707m/sec]$. The trajectories of the chaser during Phase I are shown in Figure 4. In this phase, line of sight (LOS) measurements with zero-mean Gaussian noise and variance $(0.001rad)^2$ are available every $T_s=10sec$ (representing, with some abuse of notation, y_a and σ_1^2). Also, a zero-mean Gaussian process noise with variance $(10^{-4}m/sec^2)^2$ is added to the plant dynamics in (4). The initial conditions used for the estimate of η state is $\eta(0,0) \pm [1000m \quad 1000m \quad 0m/sec \quad 0m/sec]$.

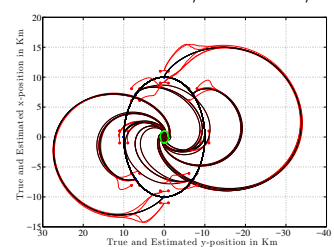


Fig. 4. Trajectories of the chaser during Phase I $(m=m_c)$

Since in Phase II-IV both ρ and α are available, the state can be easily reconstructed. Therefore, noise-free measurements are considered but a zero-mean Gaussian process noise with variance $(10^{-4}m/sec^2)^2$ is added to the plant in (4) during Phase II, IV, while during Phase III, with variance of $(10^{-6}m/sec^2)^2$. In addition, we also add very small zero-mean Gaussian residual noise (considering the best performance of a chosen filter) to the estimated position and velocity components for Phase II -IV. In the simulation results shown in Figure 5, the chaser reaches the desired neighborhood of the target in worst case time $T_1 + T_2 + T_3 \approx 2.8hr < t_e$, while maintaining the input constraint $\|u\|_{\infty} \leq 0.02m/sec^2$. The total worst case time to complete the mission is $T_1 + T_2 + T_3 + T_4 \approx 5.6hr < t_f$, which is within specifications.

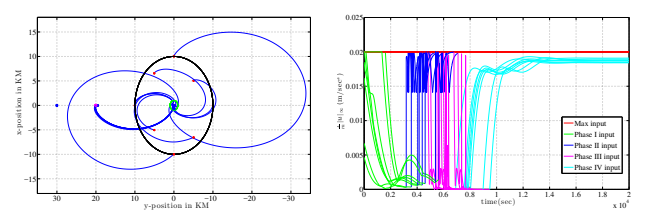


Fig. 5. Trajectories of chaser and chaser-target during Phase I-IV, with $m=m_c$ for Phase I-III, $m=m_c+m_t$ for Phase IV and control input

Due to the interesting chaser motion, we also perform multiple simulations when $\mathcal{H}_{c,2}$ is used, for initial position $(x(0,0),y(0,0))\in D_{12}$, where $D_{12}:=\{\eta\in\mathbb{R}^4:\rho(x,y)\in[0,\rho_r]\}, \rho_r=700m$, and initial velocity $\rho(\dot{x}(0,0),\dot{y}(0,0))\in[0,0.64m/s]$. Simulation results are presented in Figure 6. With $\rho^*=100m$, $\alpha^*=179deg$, and $\varrho=10deg$, the worst-case time to reach the target set was found to be $T_2\approx2500sec$. The motion of the chaser with both h=1 and h=-1 are shown in Figure 6, which highlights the capabilities conferred by the logic variable in the hybrid controller.

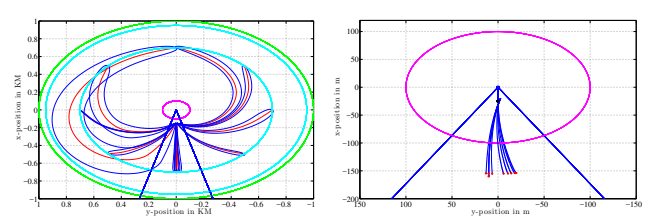


Fig. 6. Trajectories of the chaser during Phase II and Phase III $(m=m_c)$. We also show the chaser evolution during the approach/closing stage (Phase III) and highlight the specific

motion provided by our controller $\mathcal{H}_{c,3}$. Multiple simulations from $(x(0,0),y(0,0))\in\mathcal{A}_2+\delta_2\mathbb{B}$, where $\mathcal{A}_2=\{\eta\in\mathbb{R}^4: \rho=150m,\alpha=h\,179deg\}$ and $\delta_2=10m$, are presented in the Figure 6. The reference way-point, where the hybrid controller switches between subcontrollers is given by $\eta_r=[-25m\ 0m\ 0m/sec\ 0m/sec]^{\top}$. For this LQR controller, the weight matrices Q, R and other gain parameters are chosen so that the input constraint $\|u\|_{\infty}\leq 0.02m/sec^2$ is satisfied. With an estimated worst-case time to reach the target of $T_3\approx 1800sec$, the chaser reaches $\delta_3\mathbb{B}$ with $\delta_3\in[2cm,8cm]$ for several initial conditions as presented in Figure 6.

VI. CONCLUSION

For the problem of rendezvous, proximity operations, and docking of an autonomous spacecraft, we characterized the family of individual controllers and highlighted the required properties they should induce to the closed-loop system to solve the problem within each phase of operation. Particular designs for each phase/controller were proposed. Numerical results validate the approach. Current efforts focus on characterizing the margin of robustness induced by the proposed hybrid controllers, for which the first step is to perform Lyapunov analysis of the individual controllers.

REFERENCES

- W. H. Clohessy and R. S. Wiltshire. Terminal guidance system for satellite rendezvous. *Journal of the Aerospace Sciences*, 27(9):653– 658, 1960.
- [2] G. Hill. Researches in the lunar theory. American Journal of Mathematics, 1:5–26, 1878.
- [3] C. A. Kluever. Feedback control for spacecraft rendezvous and docking. *Journal of Guidance, Control, and Dynamics*, 22(4):609– 611, 1999.
- [4] M. Nazari and E. A. Butcher. Fuel efficient periodic gain control strategies for spacecraft relative motion in elliptic chief orbits. *International Journal of Dynamics and Control*, 4:104–122, 2016.
- [5] D. Lee, H. Bang, E. A. Butcher, and A. K. Sanyal. Nonlinear output tracking and disturbance rejection for autonomous close range rendezvous and docking of spacecraft. *Transactions of the Japan Society for Aeronautical and Space Sciences*, 57:225–237, 2014.
- [6] R. Vazquez, F. Gavilan, and E. F. Camacho. Trajectory planning for spacecraft rendezvous with on/off thrusters. *IFAC Proceedings Volumes*, 44(1):8473–8478, 2011.
- [7] S. Di Cairano, H. Park, and I. Kolmanovsky. Model predictive control approach for guidance of spacecraft rendezvous and proximity maneuvering. *International Journal of Robust and Nonlinear Control*, 22(12):1398–1427, 2012.
- [8] A. Weiss, M. Baldwin, R. S. Erwin, and I. Kolmanovsky. Model predictive control for spacecraft rendezvous and docking: Strategies for handling constraints and case studies. *IEEE Transactions on Control Systems Technology*, 23(4):1638–1647, 2015.
- [9] C. Jewison and R. S. Erwin. A spacecraft benchmark problem for hybrid control and estimation. To appear in Proceedings of 55th IEEE Conference on Decision and Control, 2016.
- [10] R. Ğoebel, R. G. Sanfelice, and A.R. Teel. Hybrid dynamical systems. *IEEE Control Systems Magazine*, 29(2):28–93, April 2009.
 [11] R. Goebel, R. G. Sanfelice, and A. R. Teel. *Hybrid Dynamical*
- [11] R. Goebel, R. G. Sanfelice, and A. R. Teel. Hybrid Dynamical Systems: Modeling, Stability, and Robustness. Princeton University Press, New Jersey, 2012.
- [12] D. C. Woffinden and D. K. Geller. Optimal orbital rendezvous maneuvering for angles-only navigation. *Journal of guidance, control, and dynamics*, 32(4):1382–1387, 2009.
- [13] J. Wang, E. A. Butcher, and A. T. Lovell. Use of nonlinerities for increased observability in relative orbit estimation. AAS, 15(623):04– 257, 2015.
- [14] K. Alfriend, S. R. Vadali, P. Gurfil, J. How, and L. Breger. Spacecraft formation flying: dynamics, control and navigation, volume 2. Butterworth-Heinemann. 2009.